Available online at www.sciencedirect.com
ScienceDirect
Journal of Computational Physics 218 (2006) 141–158
JOURNAL OF COMPUTATIONAL PHYSICS
www.elsevier.com/locate/jcp

Solving the volume integral equations of electromagnetic scattering

Matthys M. Botha *

Department of Electrical and Electronic Engineering, University of Stellenbosch, Private Bag X1, Matieland 7602, Stellenbosch, South Africa

Received 10 November 2005; accepted 3 February 2006
Available online 29 March 2006

Abstract

Time-harmonic electromagnetic scattering by inhomogeneous, three-dimensional structures within a free space environment can be described by electric- and magnetic field, volume integral equations involving the free space Green function. A comprehensive set of Galerkin projection formulations (also known as moment methods) for the numerical solution of these equations is presented, together with comparative numerical results. Such formulations are widely used for particle scattering analysis, optical near field calculation, etc. Results are obtained with higher-order, divergence- and curl-conforming basis functions on iso-parametric, tetrahedral meshes. The results demonstrate that all formulations converge with similar accuracy in the case of an analytically-solvable test problem. When modeling flux densities as solution variables, it is argued that solenoidal function spaces should be used, rather than the standard divergence-conforming function spaces; this assertion is supported by the results. Some of the formulations involve solving for curl-conforming fields; such fields can be discretized with fewer unknowns than divergence-conforming ones, implying lower computational costs. Additionally, some formulations yield system matrices which are approximately half-way sparse, meaning that computational costs will be down by a factor of 2 when iterative solvers are employed, which is the case for the widely-used fast methods.

Keywords: Computational electromagnetics; Volume integral equations; Galerkin projection; Method of moments; Tetrahedral basis functions; Higher-order modeling; Maxwell's equations

1. Introduction

Time-harmonic electromagnetic scattering by inhomogeneous three-dimensional (3D) structures characterized by permittivity and permiability functions $\epsilon(x, y, z)$ and $\mu(x, y, z)$, and located within a free space environment, can be described by electric- and magnetic field, volume integral equations (EF-VIE and MF-VIE) involving the free space Green function. This paper presents a set of Galerkin projection formulations for the numerical solution of these VIE's, with comparative numerical results.

* Tel.: +27 21 808 4354; fax: +27 21 808 4981.
E-mail address: mmbotha@sun.ac.za.

0021-9991/$ - see front matter
doi:10.1016/j.jcp.2006.02.004

The electromagnetic VIE's have been solved numerically by many workers over the years, with wide ranging applications. In 1984, Schaubert et al. [1] formulated the Galerkin solution of the EF-VIE for dielectric scatterers in terms of the electric flux density with conforming (Raviart–Thomas) vector basis functions, for the first time. This approach and its counterpart based on collocation (together referred to as *moment methods* [2,3]) have found wide ranging applications ever since, e.g.: particle scattering [4,5], optical near field calculation [6,7], polarizability analysis [8], indoor radio-wave propagation modeling [9], etc. Various features were added to this formulation, such as fast solvers enabling large-scale analysis (cf. [10]), coupling with surface IE's [11], low-order solenoidal basis functions to model flux densities more realistically [12,13], and a special version for low-frequency analysis [14] – but the basic projection formulation has essentially remained unchanged. The idea of solving the MF-VIE for dielectric scatterers instead (analogous to solving either the EF- or MF surface IE in the case of conducting scatterers [2]) has not received much attention, though it has been proposed in [15,16]. Moreover, VIE-based analysis of structures with inhomogeneity in both ϵ and μ has almost not been considered at all.

Given the above discussion, it is clear that numerical solutions of the electromagnetic VIE's continue to be a relevant topic, and that such methods are widely used. It is also clear that there are still some unresolved issues relating to MF-VIE-based dielectric formulations and the lack of formulations for generally inhomogeneous scatterers, which deserve attention. The main contributions of this paper relate to these issues, and are as follows:

(1) The presentation of a comprehensive set of VIE-based Galerkin formulations for dielectric, magnetic, as well as generally inhomogeneous scatterers – some of which are new, with pre-existing ones included for completeness.
(2) Comparative numerical results, using recently proposed higher-order basis functions which have the mimetic property [17] (divergence-conforming [18] and curl-conforming [19]), together with higher-order geometric representations – studying the convergences of the presented formulations.
(3) The issue of solenoidal flux representations vs. standard divergence-conforming representations is considered with comparative numerical results.

The paper is organized as follows. First, the VIE's for time-harmonic electromagnetic fields are derived in Section 2. Galerkin projection methods for their numerical solution are established in Section 3, categorized according to the material properties of the scatterer. The section concludes with discussions on symmetrization, discretization on tetrahedral grids, and solvability. Then follows numerical results in Section 4, which includes error convergence studies for all formulations and the analysis of scattering by a general object, not possessing an analytical solution. The paper ends with some conclusions.

2. Volume integral equations for electromagnetic fields

2.1. Maxwell's equations in time-harmonic form

Given a positive frequency convention $e^{j\omega t}$ ($j = \sqrt{-1}$), the 3D, time-harmonic Maxwell equations in phasor format are as follows:

$$\nabla \times \mathbf{E} = -j\omega\mathbf{B} - \mathbf{M}_{\text{src}}, \tag{1}$$

$$\nabla \times \mathbf{H} = +j\omega\mathbf{D} + \mathbf{J}_{\text{src}}, \tag{2}$$

$$\mathbf{D} = \epsilon\mathbf{E}, \tag{3}$$

$$\mathbf{B} = \mu\mathbf{H}. \tag{4}$$

At any angular frequency $\omega > 0$, this set of four equations may be solved in terms of the four quantities $\mathbf{E}$, $\mathbf{H}$ (electric- and magnetic fields), $\mathbf{D}$ and $\mathbf{B}$ (electric- and magnetic flux densities). The impressed electric- and magnetic volume current sources $\mathbf{M}_{\text{src}}$ and $\mathbf{J}_{\text{src}}$ provide the excitation. The permittivity and permeability are functions of position, and can be expressed in terms of relative values multiplied with the values in free

space (vacuum), i.e. $\epsilon = \epsilon_r\epsilon_0$ and $\mu = \mu_r\mu_0$; ϵ_r and μ_r are generally complex-valued, with real parts $\geqslant 1$. From (1) and (2) it follows that

$$\nabla \cdot \mathbf{D} = -\frac{1}{\mathrm{j}\omega}\nabla \cdot \mathbf{J}_{\mathrm{src}}; \quad \nabla \cdot \mathbf{B} = -\frac{1}{\mathrm{j}\omega}\nabla \cdot \mathbf{M}_{\mathrm{src}}. \tag{5}$$

2.2. The volume equivalence principle

The set of equations (1)–(4) can be reformulated by way of the *volume equivalence principle*, which states that field-dependent sources may be introduced into Maxwell's equations, such that an equivalent set of equations is obtained with the same field solution, but now existing in free space ($\epsilon_r = \mu_r = 1$) [20]. Start by eliminating **D** and **B** from (1) and (2), and rewrite the resulting equations as

$$\nabla \times \mathbf{E} = -\mathrm{j}\omega\mu_0\mathbf{H} - \mathbf{M}_{\mathrm{src}} - \mathrm{j}\omega\mu_0(\mu_r - 1)\mathbf{H},$$
$$\nabla \times \mathbf{H} = +\mathrm{j}\omega\epsilon_0\mathbf{E} + \mathbf{J}_{\mathrm{src}} + \mathrm{j}\omega\epsilon_0(\epsilon_r - 1)\mathbf{E}.$$

Now define the equivalent sources as

$$\mathbf{J}_{\mathrm{eq}} = \mathrm{j}\omega\epsilon_0(\epsilon_r - 1)\mathbf{E}; \quad \mathbf{M}_{\mathrm{eq}} = \mathrm{j}\omega\mu_0(\mu_r - 1)\mathbf{H}, \tag{6}$$

to obtain the new set of free space equations, with the same solution as (1)–(4):

$$\nabla \times \mathbf{E} = -\mathrm{j}\omega\mu_0\mathbf{H} - \mathbf{M}_{\mathrm{src}} - \mathbf{M}_{\mathrm{eq}}, \tag{7}$$
$$\nabla \times \mathbf{H} = +\mathrm{j}\omega\epsilon_0\mathbf{E} + \mathbf{J}_{\mathrm{src}} + \mathbf{J}_{\mathrm{eq}}. \tag{8}$$

2.3. Volume integral equations

There are well-known, integral equation representations of the solutions to Maxwell's equations in free space [21]. Given a bounded domain $\Lambda \subset \mathbb{R}^3$, define the following two integral operators:

$$\mathscr{N}(\Lambda, \mathbf{v}) \equiv \mathrm{j}k_0 \int_{\Lambda} \overline{\overline{G}}_{\mathrm{e}}(\mathbf{r}, \mathbf{r}') \cdot \mathbf{v}(\mathbf{r}')\,\mathrm{d}V', \tag{9}$$

$$\mathscr{M}(\Lambda, \mathbf{v}) \equiv -\int_{\Lambda} \overline{\overline{G}}_{\mathrm{m}}(\mathbf{r}, \mathbf{r}') \cdot \mathbf{v}(\mathbf{r}')\,\mathrm{d}V', \tag{10}$$

where the free space, dyadic Green functions of electric- and magnetic types are defined as

$$\overline{\overline{G}}_{\mathrm{e}}(\mathbf{r}, \mathbf{r}') \equiv \left(\overline{\overline{I}} - \frac{1}{k_0^2}\nabla\,\nabla'\right) G_0(\mathbf{r}, \mathbf{r}'); \quad \overline{\overline{G}}_{\mathrm{m}}(\mathbf{r}, \mathbf{r}') \equiv \nabla G_0(\mathbf{r}, \mathbf{r}') \times \overline{\overline{I}}. \tag{11}$$

Here, $G_0(\mathbf{r}, \mathbf{r}') \equiv \mathrm{e}^{-\mathrm{j}k_0|\mathbf{r}-\mathbf{r}'|}/4\pi|\mathbf{r} - \mathbf{r}'|$ denotes the free space scalar Green function.

Now suppose that $\mathbf{J}_{\mathrm{src}} \neq 0$ on Λ, is an arbitrary enforced electric current distribution in free space, then the resulting electromagnetic fields can be obtained as follows:

$$\mathbf{E}(\mathbf{r}) = -Z_0\mathscr{N}(\Lambda, \mathbf{J}_{\mathrm{src}}); \quad \mathbf{H}(\mathbf{r}) = -\mathscr{M}(\Lambda, \mathbf{J}_{\mathrm{src}}); \qquad \mathbf{r} \in \mathbb{R}^3, \tag{12}$$

where $k_0 = \omega/c_0$ and $Z_0 = \sqrt{\mu_0/\epsilon_0}$ denote the free space wave-number and wave-impedance, respectively.

Now consider the equivalent free space system (7), (8). Suppose that $\epsilon_r \neq 1$ and $\mu_r \neq 1$ on a bounded domain $\Omega \subset \mathbb{R}^3$. The VIE's for general, inhomogeneous scatterers follow by duality from (12), as

$$\mathbf{E} = \mathbf{E}_{\mathrm{inc}} - Z_0\mathscr{N}(\Omega, \mathbf{J}_{\mathrm{eq}}) + \mathscr{M}(\Omega, \mathbf{M}_{\mathrm{eq}}), \tag{13}$$

$$\mathbf{H} = \mathbf{H}_{\mathrm{inc}} - \mathscr{M}(\Omega, \mathbf{J}_{\mathrm{eq}}) - \frac{1}{Z_0}\mathscr{N}(\Omega, \mathbf{M}_{\mathrm{eq}}), \tag{14}$$

where the effects of the true sources $\mathbf{J}_{\mathrm{src}}$ and $\mathbf{M}_{\mathrm{src}}$ were consolidated into the incident field terms $\mathbf{E}_{\mathrm{inc}}$ and $\mathbf{H}_{\mathrm{inc}}$. These two equations will be called the EF-VIE and MF-VIE, respectively; their numerical solution via Galerkin projection is the subject of the rest of this paper.

As an aside, observe that $\mathscr{N}(\cdot,\cdot)$ is hypersingular, and therefore requires special attention when evaluating the fields inside the source region, as discussed by various authors (cf. [2,21]). This issue will not be dealt with here, since the hypersingularity vanishes in all the numerical formulations to be presented.

3. VIE-based, Galerkin projection methods

This section formulates the numerical solution of the EF- and MF-VIE's by way of the Galerkin projection method [22]. In order to formulate a Galerkin projection method, one needs to choose the equation(s) to solve, the solution variable(s) and associated function space(s). A comprehensive set of formulations will be presented, each catering for a specific combination of scatterer-type and solution variable(s). The various possible solution variables will first be discussed, followed by the various possible formulations, classified with respect to dielectric, magnetic, or general scatterers. The section ends with discussions on symmetrization, discretization and solvability.

3.1. Solution variables and function spaces

From power conservation arguments [23], it follows that the physical electromagnetic quantities **E**, **D**, **H** and **B** are square integrable in $\mathbb{R}^3$, and therefore also in Ω. Specifically, if the incident fields in the EF- and MF-VIE are required to relate to solenoidal sources $\nabla\cdot\mathbf{J}_{\text{src}} = \nabla\cdot\mathbf{M}_{\text{src}} = 0$ (see (5)), then

$$\mathbf{E},\mathbf{H}\in V_{\text{curl}};\quad \mathbf{D},\mathbf{B}\in V_{\text{div},0} \tag{15}$$

with

$$V_{\text{curl}} = \{\mathbf{v}\in H(\text{curl},\Omega)\};\quad V_{\text{div},0} = \{\mathbf{v}\in H(\text{div},\Omega)\,|\,\nabla\cdot\mathbf{v}=0\}, \tag{16}$$

where $H(\text{curl},\Omega)$ and $H(\text{div},\Omega)$ denote the spaces of vector functions, which together with their curls and divergences, respectively, are square integrable on Ω (i.e. curl- and divergence-conforming functions).

The VIE's are stated in terms of the physical electromagnetic quantities on the one hand, and the equivalent currents on the other. Since there exists simple, linear relationships between these two sets of quantities, it follows that one may equally well endeavour to solve the VIE's in terms of either set. However, the equivalent currents are linear combinations of curl- and divergence-conforming quantities and as such are non-conforming, implying larger solution spaces. Thus, it is more favorable to solve the VIE's in terms of the physical electromagnetic quantities. The equivalent sources may be expressed as $\mathbf{J}_{\text{eq}} = \text{j}\omega\chi_\epsilon\mathbf{D}$ and $\mathbf{M}_{\text{eq}} = \text{j}\omega\chi_\mu\mathbf{B}$, where

$$\chi_\epsilon = \frac{\epsilon_r-1}{\epsilon_r};\quad \chi_\mu = \frac{\mu_r-1}{\mu_r} \tag{17}$$

denote the electric and magnetic contrast ratios, to be employed later-on.

3.2. Testing the integral operators

Formulating Galerkin projection methods for the VIE's imply evaluating the complex-valued L^2-inner products of suitable testing functions, with the integral operators $\mathscr{N}(\cdot,\cdot)$ and $\mathscr{M}(\cdot,\cdot)$ applied to suitable expansion functions. In this section the appropriate choices are determined and the resolution of the hypersingularity in $\mathscr{N}(\cdot,\cdot)$ is established.

Let **a** and **b** denote arbitrary testing and expansion functions with domains of support A and B, respectively. Consider the testing of $\mathscr{N}(\cdot,\cdot)$ first. To resolve the hypersingularity of order $1/R^3$, transfer the gradient-operators away from the Green function by one or two successive applications of Gauss' Theorem. This yields the following three possibilities:

$$\begin{aligned}\int_A \mathbf{a}\cdot\mathscr{N}(B,\mathbf{b})\,\mathrm{d}V &= \mathrm{j}k_0\int_A\int_B \mathbf{a}(\mathbf{r})\cdot G_0(\mathbf{r},\mathbf{r}')\mathbf{b}(\mathbf{r}')\,\mathrm{d}V'\,\mathrm{d}V + \frac{\mathrm{j}}{k_0}\int_A\int_B \mathbf{a}(\mathbf{r})\cdot\nabla G_0(\mathbf{r},\mathbf{r}')\nabla'\cdot\mathbf{b}(\mathbf{r}')\,\mathrm{d}V'\,\mathrm{d}V\\ &\quad -\frac{\mathrm{j}}{k_0}\int_A\oint_{\partial B}\mathbf{a}(\mathbf{r})\cdot\nabla G_0(\mathbf{r},\mathbf{r}')\hat{n}'\cdot\mathbf{b}(\mathbf{r}')\mathrm{d}S'\,\mathrm{d}V\\ &= \mathrm{j}k_0\int_A\int_B \mathbf{a}(\mathbf{r})\cdot G_0(\mathbf{r},\mathbf{r}')\mathbf{b}(\mathbf{r}')\,\mathrm{d}V'\,\mathrm{d}V + \frac{\mathrm{j}}{k_0}\int_A\int_B \nabla\cdot\mathbf{a}(\mathbf{r})\nabla' G_0(\mathbf{r},\mathbf{r}')\cdot\mathbf{b}(\mathbf{r}')\,\mathrm{d}V'\,\mathrm{d}V\\ &\quad -\frac{\mathrm{j}}{k_0}\oint_{\partial A}\int_B \hat{n}\cdot\mathbf{a}(\mathbf{r})\nabla' G_0(\mathbf{r},\mathbf{r}')\cdot\mathbf{b}(\mathbf{r}')\,\mathrm{d}V'\,\mathrm{d}S\\ &= \mathrm{j}k_0\int_A\int_B \mathbf{a}(\mathbf{r})\cdot G_0(\mathbf{r},\mathbf{r}')\mathbf{b}(\mathbf{r}')\,\mathrm{d}V'\,\mathrm{d}V - \frac{\mathrm{j}}{k_0}\int_A\int_B \nabla\cdot\mathbf{a}(\mathbf{r})G_0(\mathbf{r},\mathbf{r}')\nabla'\cdot\mathbf{b}(\mathbf{r}')\,\mathrm{d}V'\,\mathrm{d}V\\ &\quad +\frac{\mathrm{j}}{k_0}\oint_{\partial A}\int_B \hat{n}\cdot\mathbf{a}(\mathbf{r})G_0(\mathbf{r},\mathbf{r}')\nabla'\cdot\mathbf{b}(\mathbf{r}')\,\mathrm{d}V'\,\mathrm{d}S + \frac{\mathrm{j}}{k_0}\int_A\oint_{\partial B}\nabla\cdot\mathbf{a}(\mathbf{r})G_0(\mathbf{r},\mathbf{r}')\hat{n}'\cdot\mathbf{b}(\mathbf{r}')\,\mathrm{d}S'\,\mathrm{d}V\\ &\quad -\frac{\mathrm{j}}{k_0}\oint_{\partial A}\oint_{\partial B}\hat{n}\cdot\mathbf{a}(\mathbf{r})G_0(\mathbf{r},\mathbf{r}')\hat{n}'\cdot\mathbf{b}(\mathbf{r}')\,\mathrm{d}S'\,\mathrm{d}S. \end{aligned}\tag{18}$$

From this result it is clear that either the expansion or testing function for $\mathscr{N}(\cdot,\cdot)$ must at least be divergence-conforming. This places some restrictions on the construction of numerical methods. It is also clear that when the testing and expansion functions are the same, the contribution of the singularity will be properly tested. The third form is the easiest to evaluate numerically, because its weak singularity ($1/R$) is one order lower than those in the first and second forms (i.e. $1/R^2$), however, both expansion and testing functions are required to be divergence-conforming in the case of the third form.

Next consider the testing of $\mathscr{M}(\cdot,\cdot)$:

$$\int_A \mathbf{a}\cdot\mathscr{M}(B,\mathbf{b})\,\mathrm{d}V = \int_A\int_B \mathbf{a}(\mathbf{r})\cdot\nabla' G_0(\mathbf{r},\mathbf{r}')\times\mathbf{b}(\mathbf{r}')\,\mathrm{d}V'\,\mathrm{d}V.\tag{19}$$

In this case the operator is weakly singular (of order $1/R^2$) and there are no requirements on the conformity of the testing and expansion functions. However, note that as a consequence of the cross product in the kernel, the singularity will make no contribution when the testing and expansion functions are the same.

3.3. Formulations for dielectric scatterers

For a dielectric scatterer, $\mathbf{M}_{\mathrm{eq}} = 0$. First consider solving the EF-VIE. Of the four possible solution variables, only **D** is suitable. To see this, consider the other three: **E** is unacceptable because either the argument or the testing function of $\mathscr{N}(\cdot,\cdot)$ must be divergence-conforming (see Section 3.2); **B** will not work, because then the curl of a divergence-conforming quantity will be required to obtain **E**; finally, **H** is also not feasible, since it will only feature as $\nabla\times\mathbf{H}$, which is not uniquely solvable. The Galerkin approach involves using the same function space for testing, as for expansion, it follows that divergence-conforming testing is required in the case of **D**. The resulting formulation is

$$\begin{cases} \text{Formulation D.1 : } \textit{Find } \mathbf{D}\in V_{\mathrm{div},0} \textit{ such that}\\ \qquad B(\mathbf{D},\mathbf{V}) = L(\mathbf{V}) \quad \forall\ \mathbf{V}\in V_{\mathrm{div},0}\\ \textit{with}\\ \qquad B(\mathbf{D},\mathbf{V}) = \displaystyle\int_\Omega\left[\frac{\mathbf{D}}{\epsilon_r\epsilon_0} + Z_0\mathscr{N}(\Omega,\mathrm{j}\omega\chi_\epsilon\mathbf{D})\right]\cdot\mathbf{V}\,\mathrm{d}V,\\ \qquad L(\mathbf{V}) = \displaystyle\int_\Omega \mathbf{E}_{\mathrm{inc}}\cdot\mathbf{V}\,\mathrm{d}V. \end{cases}\tag{20}$$

Now consider solving the MF-VIE. In this case **H** is the only appropriate solution variable. Both **D** and **B** are unacceptable, since either will lead to taking the curl of a divergence-conforming function. **E** is not an option, due to the issue of poor testing, as described in Section 3.2. The resulting formulation is

$$\begin{cases} \text{Formulation D.2}: \ \textit{Find } \mathbf{H} \in V_{\text{curl}} \textit{ such that} \\ \quad B(\mathbf{H},\mathbf{W}) = L(\mathbf{W}) \quad \forall\ \mathbf{W} \in V_{\text{curl}} \\ \textit{with} \\ \quad B(\mathbf{H},\mathbf{W}) = \displaystyle\int_\Omega [\mathbf{H} + \mathscr{M}(\Omega, \chi_\epsilon \nabla \times \mathbf{H})] \cdot \mathbf{W}\, \mathrm{d}V, \\ \quad L(\mathbf{W}) = \displaystyle\int_\Omega \mathbf{H}_{\text{inc}} \cdot \mathbf{W}\, \mathrm{d}V. \end{cases} \tag{21}$$

The EF-VIE formulation has been widely used in the past, but most often with the general divergence-conforming solution space $V_{\text{div}} = \{\mathbf{v} \in H(\text{div}, \Omega)\}$. The current form of the MF-VIE formulation has now been presented for the first time – the MF-VIE has been expressed in terms of the **H**-field in the past [15,16], but its subsequent solution via Galerkin projection onto a curl-conforming solution space (i.e. formulation (21)) has not been presented before, to the author's knowledge.

3.4. Formulations for magnetic scatterers

In this case $\mathbf{J}_{\text{eq}} = 0$. By duality, one obtains two formulations similar to those proposed for the dielectric scatterer, but now in terms of the solution variables **B** and **E**, as follows:

$$\begin{cases} \text{Formulation M.1}: \ \textit{Find } \mathbf{B} \in V_{\text{div},0} \textit{ such that} \\ \quad B(\mathbf{B},\mathbf{V}) = L(\mathbf{V}) \quad \forall\ \mathbf{V} \in V_{\text{div},0} \\ \textit{with} \\ \quad B(\mathbf{B},\mathbf{V}) = \displaystyle\int_\Omega \left[\frac{\mathbf{B}}{\mu_r \mu_0} + \frac{1}{Z_0}\mathscr{N}(\Omega, \mathrm{j}\omega\chi_\mu \mathbf{B})\right] \cdot \mathbf{V}\, \mathrm{d}V, \\ \quad L(\mathbf{V}) = \displaystyle\int_\Omega \mathbf{H}_{\text{inc}} \cdot \mathbf{V}\, \mathrm{d}V. \end{cases} \tag{22}$$

$$\begin{cases} \text{Formulation M.2}: \ \textit{Find } \mathbf{E} \in V_{\text{curl}} \textit{ such that} \\ \quad B(\mathbf{E},\mathbf{W}) = L(\mathbf{W}) \quad \forall\ \mathbf{W} \in V_{\text{curl}} \\ \textit{with} \\ \quad B(\mathbf{E},\mathbf{W}) = \displaystyle\int_\Omega [\mathbf{E} - \mathscr{M}(\Omega, -\chi_\mu \nabla \times \mathbf{E})] \cdot \mathbf{W}\, \mathrm{d}V, \\ \quad L(\mathbf{W}) = \displaystyle\int_\Omega \mathbf{E}_{\text{inc}} \cdot \mathbf{W}\, \mathrm{d}V. \end{cases} \tag{23}$$

3.5. Formulations for general scatterers

In the case of a generally inhomogeneous scatterer, both $\mathbf{J}_{\text{eq}}$ and $\mathbf{M}_{\text{eq}}$ are present. A straightforward extension of the standard formulations (20) and (22) is to solve the EF-VIE and MF-VIE simultaneously, with $\mathbf{J}_{\text{eq}} = \mathrm{j}\omega\chi_\epsilon \mathbf{D}$ and $\mathbf{M}_{\text{eq}} = \mathrm{j}\omega\chi_\mu \mathbf{B}$, i.e.

$$\begin{cases} \text{Formulation G.1}: \ \textit{Find } [\mathbf{D},\mathbf{B}] \in V_{\text{div},0} \times V_{\text{div},0} \textit{ such that} \\ \quad B([\mathbf{D},\mathbf{B}],[\mathbf{V},\mathbf{X}]) = L([\mathbf{V},\mathbf{X}]) \quad \forall\ [\mathbf{V},\mathbf{X}] \in V_{\text{div},0} \times V_{\text{div},0} \\ \textit{with} \\ \quad B([\mathbf{D},\mathbf{B}],[\mathbf{V},\mathbf{X}]) = \displaystyle\int_\Omega \left[\frac{\mathbf{D}}{\epsilon_r \epsilon_0} + Z_0 \mathscr{N}(\Omega, \mathrm{j}\omega\chi_\epsilon \mathbf{D}) - \mathscr{M}\left(\Omega, \mathrm{j}\omega\chi_\mu \mathbf{B}\right)\right] \cdot \mathbf{V}\, \mathrm{d}V \\ \qquad\qquad\qquad - \displaystyle\int_\Omega \left[\frac{\mathbf{B}}{\mu_r \mu_0} + \frac{1}{Z_0}\mathscr{N}\left(\Omega, \mathrm{j}\omega\chi_\mu \mathbf{B}\right) + \mathscr{M}(\Omega, \mathrm{j}\omega\chi_\epsilon \mathbf{D})\right] \cdot \mathbf{X}\, \mathrm{d}V, \\ \quad L([\mathbf{V},\mathbf{X}]) = \displaystyle\int_\Omega \mathbf{E}_{\text{inc}} \cdot \mathbf{V}\, \mathrm{d}V - \int_\Omega \mathbf{H}_{\text{inc}} \cdot \mathbf{X}\, \mathrm{d}V. \end{cases} \tag{24}$$

Taking a cue from formulations (21) and (23), the two VIE's may also be simultaneously solved with the substitutions $\mathbf{J}_{\text{eq}} = \chi_\epsilon \nabla \times \mathbf{H}$ and $\mathbf{M}_{\text{eq}} = -\chi_\mu \nabla \times \mathbf{E}$, yielding

$$\left\{\begin{array}{l} \text{Formulation G.2: } \textit{Find } [\mathbf{E},\mathbf{H}] \in V_{\text{curl}} \times V_{\text{curl}} \textit{ such that} \\ \quad B([\mathbf{E},\mathbf{H}],[\mathbf{W},\mathbf{Y}]) = L([\mathbf{W},\mathbf{Y}]) \quad \forall\ [\mathbf{W},\mathbf{Y}] \in V_{\text{curl}} \times V_{\text{curl}} \\ \textit{with} \\ \quad B([\mathbf{E},\mathbf{H}],[\mathbf{W},\mathbf{Y}]) = \displaystyle\int_\Omega [\mathbf{E} + Z_0 \mathscr{N}(\Omega, \chi_\epsilon \nabla \times \mathbf{H}) - \mathscr{M}(\Omega, -\chi_\mu \nabla \times \mathbf{E})] \cdot \mathbf{W}\, \mathrm{d}V \\ \qquad\qquad + \displaystyle\int_\Omega [\mathbf{H} + \frac{1}{Z_0} \mathscr{N}(\Omega, -\chi_\mu \nabla \times \mathbf{E}) + \mathscr{M}(\Omega, \chi_\epsilon \nabla \times \mathbf{H})] \cdot \mathbf{Y}\, \mathrm{d}V, \\ \quad L([\mathbf{W},\mathbf{Y}]) = \displaystyle\int_\Omega \mathbf{E}_{\text{inc}} \cdot \mathbf{W}\, \mathrm{d}V + \int_\Omega \mathbf{H}_{\text{inc}} \cdot \mathbf{Y}\, \mathrm{d}V. \end{array}\right. \tag{25}$$

Note that in both the above formulations all self-interactions are properly tested. Further observe that the MF-VIE has been scaled by -1 in (24), to facilitate symmetrization, to be discussed later-on. Concerning formulation (25): the first form of $\mathscr{N}(\cdot,\cdot)$-testing (18) must be used here, since the testing functions are not divergence-conforming, while the operator argument is ($\nabla \times \mathbf{v} \in V_{\text{div},0}\ \forall\ \mathbf{v} \in V_{\text{curl}}$).

One can also formulate methods in terms of a single integral equation. Consider the EF-VIE first. With the substitutions $\mathbf{J}_{\text{eq}} = \mathrm{j}\omega\chi_\epsilon \mathbf{D}$ and $\mathbf{M}_{\text{eq}} = -\chi_\mu \nabla \times \mathbf{E}$, the EF-VIE may be solved together with the electric field constitutive relation (3) in two possible ways, yielding the following two formulations:

$$\left\{\begin{array}{l} \text{Formulation G.3: } \textit{Find } [\mathbf{D},\mathbf{E}] \in V_{\text{div},0} \times V_{\text{curl}} \textit{ such that} \\ \quad B([\mathbf{D},\mathbf{E}],[\mathbf{V},\mathbf{W}]) = L([\mathbf{V},\mathbf{W}]) \quad \forall\ [\mathbf{V},\mathbf{W}] \in V_{\text{div},0} \times V_{\text{curl}} \\ \textit{with} \\ \quad B([\mathbf{D},\mathbf{E}],[\mathbf{V},\mathbf{W}]) = \displaystyle\int_\Omega \left[\frac{\mathbf{D}}{\epsilon_r\epsilon_0} + Z_0 \mathscr{N}(\Omega, \mathrm{j}\omega\chi_\epsilon \mathbf{D}) - \mathscr{M}(\Omega, -\chi_\mu \nabla \times \mathbf{E})\right] \cdot \mathbf{V}\, \mathrm{d}V \\ \qquad\qquad + \displaystyle\int_\Omega \left[-\frac{\mathbf{D}}{\epsilon_r\epsilon_0} + \mathbf{E}\right] \cdot \mathbf{W}\, \mathrm{d}V, \\ \quad L([\mathbf{V},\mathbf{W}]) = \displaystyle\int_\Omega \mathbf{E}_{\text{inc}} \cdot \mathbf{V}\, \mathrm{d}V. \end{array}\right. \tag{26}$$

$$\left\{\begin{array}{l} \text{Formulation G.4: } \textit{Find } [\mathbf{E},\mathbf{D}] \in V_{\text{curl}} \times V_{\text{div},0} \textit{ such that} \\ \quad B([\mathbf{E},\mathbf{D}],[\mathbf{W},\mathbf{V}]) = L([\mathbf{W},\mathbf{V}]) \quad \forall\ [\mathbf{W},\mathbf{V}] \in V_{\text{curl}} \times V_{\text{div},0} \\ \textit{with} \\ \quad B([\mathbf{E},\mathbf{D}],[\mathbf{W},\mathbf{V}]) = \displaystyle\int_\Omega [\mathbf{E} + Z_0 \mathscr{N}(\Omega, \mathrm{j}\omega\chi_\epsilon \mathbf{D}) - \mathscr{M}(\Omega, -\chi_\mu \nabla \times \mathbf{E})] \cdot \mathbf{W}\, \mathrm{d}V \\ \qquad\qquad + \displaystyle\int_\Omega \left[\frac{\mathbf{D}}{\epsilon_r\epsilon_0} - \mathbf{E}\right] \cdot \mathbf{V}\, \mathrm{d}V, \\ \quad L([\mathbf{W},\mathbf{V}]) = \displaystyle\int_\Omega \mathbf{E}_{\text{inc}} \cdot \mathbf{W}\, \mathrm{d}V. \end{array}\right. \tag{27}$$

Two similar formulations, based on the MF-VIE and the magnetic field constitutive relation (4) may also be established, i.e.

$$\left\{\begin{array}{l} \text{Formulation G.5: } \textit{Find } [\mathbf{B},\mathbf{H}] \in V_{\text{div},0} \times V_{\text{curl}} \textit{ such that} \\ \quad B([\mathbf{B},\mathbf{H}],[\mathbf{V},\mathbf{W}]) = L([\mathbf{V},\mathbf{W}]) \quad \forall\ [\mathbf{V},\mathbf{W}] \in V_{\text{div},0} \times V_{\text{curl}} \\ \textit{with} \\ \quad B([\mathbf{B},\mathbf{H}],[\mathbf{V},\mathbf{W}]) = \displaystyle\int_\Omega \left[\frac{\mathbf{B}}{\mu_r\mu_0} + \frac{1}{Z_0} \mathscr{N}(\Omega, \mathrm{j}\omega\chi_\mu \mathbf{B}) + \mathscr{M}(\Omega, \chi_\epsilon \nabla \times \mathbf{H})\right] \cdot \mathbf{V}\, \mathrm{d}V \\ \qquad\qquad + \displaystyle\int_\Omega \left[-\frac{\mathbf{B}}{\mu_r\mu_0} + \mathbf{H}\right] \cdot \mathbf{W}\, \mathrm{d}V, \\ \quad L([\mathbf{V},\mathbf{W}]) = \displaystyle\int_\Omega \mathbf{H}_{\text{inc}} \cdot \mathbf{V}\, \mathrm{d}V. \end{array}\right. \tag{28}$$

$$\begin{cases} \text{Formulation G.6}: \ \textit{Find}\ [\mathbf{H},\mathbf{B}] \in V_{\text{curl}} \times V_{\text{div},0}\ \textit{such that} \\ \quad B([\mathbf{H},\mathbf{B}],[\mathbf{W},\mathbf{V}]) = L([\mathbf{W},\mathbf{V}]) \quad \forall\ [\mathbf{W},\mathbf{V}] \in V_{\text{curl}} \times V_{\text{div},0} \\ \textit{with} \\ \quad B([\mathbf{H},\mathbf{B}],[\mathbf{W},\mathbf{V}]) = \displaystyle\int_\Omega \left[\mathbf{H} + \frac{1}{Z_0}\mathscr{N}(\Omega, \mathrm{j}\omega\chi_\mu \mathbf{B}) + \mathscr{M}(\Omega, \chi_\epsilon \nabla\times\mathbf{H})\right]\cdot\mathbf{W}\,\mathrm{d}V \\ \qquad\qquad\qquad\qquad + \displaystyle\int_\Omega \left[\frac{\mathbf{B}}{\mu_r\mu_0} - \mathbf{H}\right]\cdot\mathbf{V}\,\mathrm{d}V, \\ \quad L([\mathbf{W},\mathbf{V}]) = \displaystyle\int_\Omega \mathbf{H}_{\text{inc}}\cdot\mathbf{W}\,\mathrm{d}V. \end{cases} \tag{29}$$

3.6. Symmetrization

From (18) and (19) and the definitions of the dyadic Green functions, it is clear that the tested integral operators possess the following symmetry properties:

$$\int_A \mathbf{a}\cdot\mathscr{N}(B,\mathbf{b})\,\mathrm{d}V = \int_B \mathbf{b}\cdot\mathscr{N}(A,\mathbf{a})\,\mathrm{d}V; \quad \int_A \mathbf{a}\cdot\mathscr{M}(B,\mathbf{b})\,\mathrm{d}V = \int_B \mathbf{b}\cdot\mathscr{M}(A,\mathbf{a})\,\mathrm{d}V. \tag{30}$$

It follows that formulations (20), (22), and (24) may be symmetrized by scaling the testing functions with the contrast functions of (17), i.e. solving

$$\text{Formulation D.1 (20)}: B(\mathbf{D},\chi_\epsilon\mathbf{V}) = L(\chi_\epsilon\mathbf{V}), \tag{31}$$

$$\text{Formulation M.1 (22)}: B(\mathbf{B},\chi_\mu\mathbf{V}) = L(\chi_\mu\mathbf{V}), \tag{32}$$

$$\text{Formulation G.1 (24)}: B([\mathbf{D},\mathbf{B}],[\chi_\epsilon\mathbf{V},\chi_\mu\mathbf{X}]) = L([\chi_\epsilon\mathbf{V},\chi_\mu\mathbf{X}]) \tag{33}$$

instead. The above bilinear forms are symmetric with respect to testing and expansion functions. For formulation (20), this kind of symmetrization has been proposed in [24].

The remaining formulations are not symmetrizable in this manner, and symmetrization will not be further explored here.

3.7. Discretization

In order to solve the proposed formulations numerically, the infinite-dimensional solution spaces $V_{\text{div},0}$ and V_{curl} must be approximated by suitable finite-dimensional sub-spaces. The finite element procedure followed here to obtain these sub-spaces entails dividing the problem domain Ω into a mesh of tetrahedral elements and then employing conforming vector basis functions on each element.

In the case of V_{curl}, the hierarchical, mixed- and full-order, curl-conforming basis functions proposed in [19] are used.

In the case of $V_{\text{div},0}$, the hierarchical, divergence-conforming, solenoidal basis functions proposed in [18] are used. Note that in order to obtain the zeroth-order solenoidal basis functions, a tree–cotree decomposition must be performed on the set of global mesh edges, as described in [18,25].

A special case arises regarding formulations (20) and (22), since the larger solution space V_{div} has traditionally been used here [1,13]. For this historical reason, it will also be considered when evaluating these formulations later on, even though such an approach constitutes a "variational crime" [26]. The space V_{div} can be represented by the full- and mixed-order, divergence-conforming basis functions, also proposed in [18].

Iso-parametric elemental geometric representations are employed, i.e. the order of geometric representation is matched with the order of the basis functions (leading to curviliear representations for orders above one). An exception is made in the case of the zeroth-order solenoidal basis functions: here a super-parametric, first-order geometric representation will be used.

Finally, observe that all of these discrete field representations have the mimetic property [17], and except for the zeroth-order solenoidal basis functions, are Nédélec-compliant [27,28] – as discussed in the references.

3.8. Solvability

Both the EF-VIE and MF-VIE are second-kind Fredholm integral equations. Unfortunately, it has been shown that the integral operator $\mathscr{N}(\cdot,\cdot)$ is not compact [29]. Therefore, the standard apparatus (cf. [22,30]) for determining the conditions under which these formulations will yield uniquely convergent solutions, does not directly apply. Here the error convergence will be studied numerically, as has been suggested in other cases [31].

4. Numerical results

The accuracy of the proposed formulations will now be evaluated numerically. Error convergence is considered in the context of sphere scattering, where analytical results are available, as is standard practice [31]. Subsequently, scattering by a general object is calculated and compared with results obtained with an independent numerical scheme.

4.1. Integrated RCS error convergence

In this section, results obtained with the various formulations will be presented for the error in the bistatic radar cross section (RCS), integrated over the unit sphere (i.e. the maximum solid angle), and normalized with respect to the true RCS. This error quantity is defined as follows:

$$\varepsilon_\sigma = \frac{\|\sigma(\theta,\phi) - \tilde{\sigma}(\theta,\phi)\|_{L^2(\Upsilon)}}{\|\sigma(\theta,\phi)\|_{L^2(\Upsilon)}}, \tag{34}$$

where $\sigma(\theta,\phi)$ and $\tilde{\sigma}(\theta,\phi)$ represent the exact and calculated bistatic RCS, respectively; and Υ represents the unit sphere surface. The bistatic RCS is defined as

$$\sigma(\theta,\phi) \equiv \lim_{r\to\infty} 4\pi r^2 \frac{|\mathbf{E}_{\text{scat}}(r,\theta,\phi)|^2}{|\mathbf{E}_{\text{inc}}|^2}, \tag{35}$$

where the scattered field $\mathbf{E}_{\text{scat}}$ is calculated with the EF-VIE in the case of $\tilde{\sigma}$.

4.1.1. Formulations for dielectric and magnetic scatterers

Only results from the formulations for dielectric scatterers will be presented, since the magnetic scatterer formulations are the duals of these. The test problem is a homogeneous unit sphere ($r_0 = 1$ m) with material parameters $\epsilon_r = 2$ and $\mu_r = 1$. The structure is exited with a plane wave at $\lambda_0 = 10$ m.

Consider formulation (20) first. Here the solution space is required to be $V_{\text{div},0}$, but the larger space V_{div} will also be considered, for the historical reason noted above. Fig. 1 shows the integrated RCS error as a function of both mesh size, and degrees of freedom, when using zeroth-, first- and second-order solenoidal basis functions. Asymptotic convergence behaviour can be observed. It is interesting that the zeroth- and first-order elements perform similarly, making the zeroth-order ones more attractive in terms of degrees of freedom. This might be due to their super-parametric characteristic. Fig. 2 shows the same set of results, but obtained with the solution space V_{div} instead — mixed- and full order, divergence-conforming basis functions of first- and second-orders are employed. In this case, the convergence behaviour is somewhat erratic as compared to the solenoidal results, which could relate to the fact that non-physical, non-solenoidal components are now being included in the solution space [12]. These non-physical components lead to the presence of a spurious charge distribution in the problem domain.

Now consider formulation (21). In Fig. 3 the same set of results is presented as above. The solution space is now V_{curl}, and is discretized with mixed- and full order, curl-conforming basis functions of first- and second-orders. Here, the mixed- and full-order elements give almost identical results in terms of accuracy, but with less degrees of freedom in the mixed-order case. For non-smooth problems, one may expect superior accuracy from the full-order elements, as discussed in the context of curl-conforming, electromagnetic, finite element analysis, in [19,32].

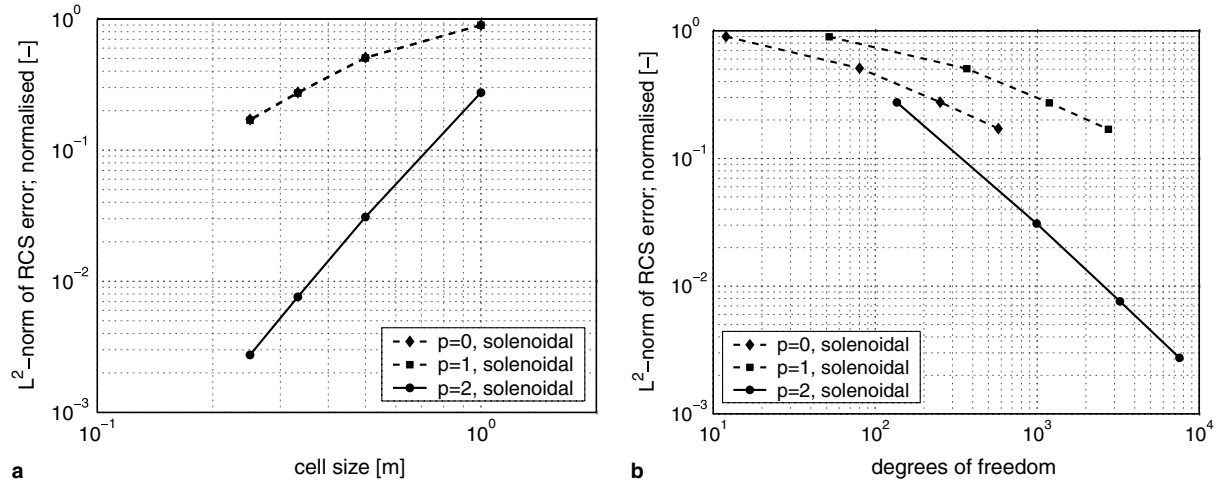

Fig. 1. RCS error convergence for formulation (20), using solenoidal divergence-conforming basis functions: (a) RCS error vs. cell size; (b) RCS error vs. degrees of freedom.

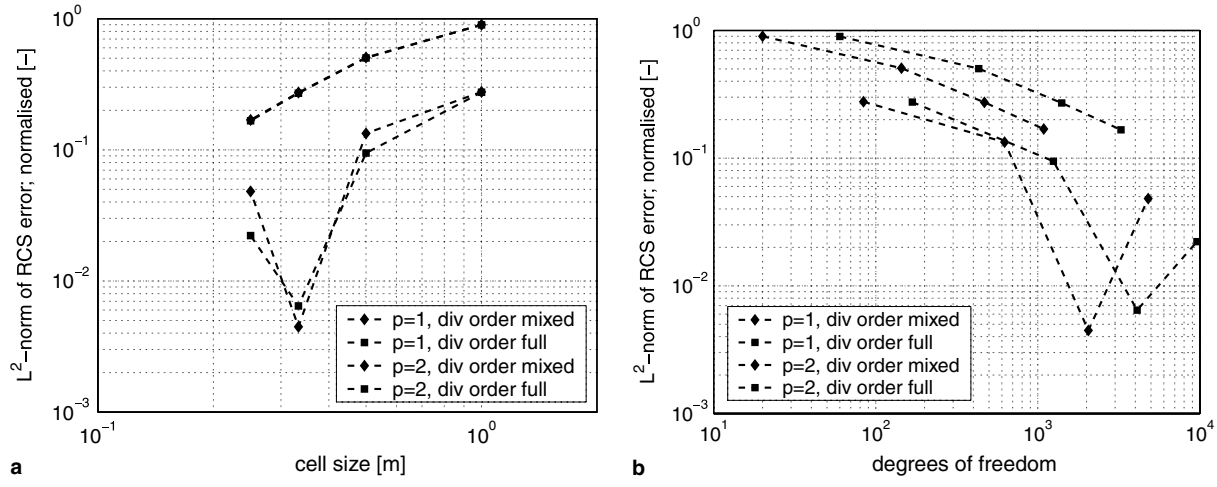

Fig. 2. RCS error convergence for formulation (20), using standard divergence-conforming basis functions: (a) RCS error vs. cell size; (b) RCS error vs. degrees of freedom.

Looking at all of these results together, some preliminary conclusions can be drawn:

(1) The solenoidal solution space $V_{\mathrm{div},0}$ should indeed be used when modeling **D** or **B**, rather than the widely-used V_{div}.
(2) Either mixed- or full-order, curl-conforming approximations may be used to approximate V_{curl}, when modeling **E** or **H**.
(3) For the same order of approximation, it appears that the new formulations based on $\mathscr{M}(\cdot,\cdot)$ are more accurate *per degree of freedom*, than those based on $\mathscr{N}(\cdot,\cdot)$. This makes sense, since the connectivity of the curl-conforming degrees of freedom is higher than that of the divergence-conforming ones, resulting in less global degrees of freedom in the former case.

4.1.2. Formulations for general scatterers

Regarding the modeling of divergence-conforming quantities in this section: Consideration will not be given to replacing $V_{\mathrm{div},0}$ with V_{div}, since this has already been shown to be disadvantageous. Also, zeroth-order

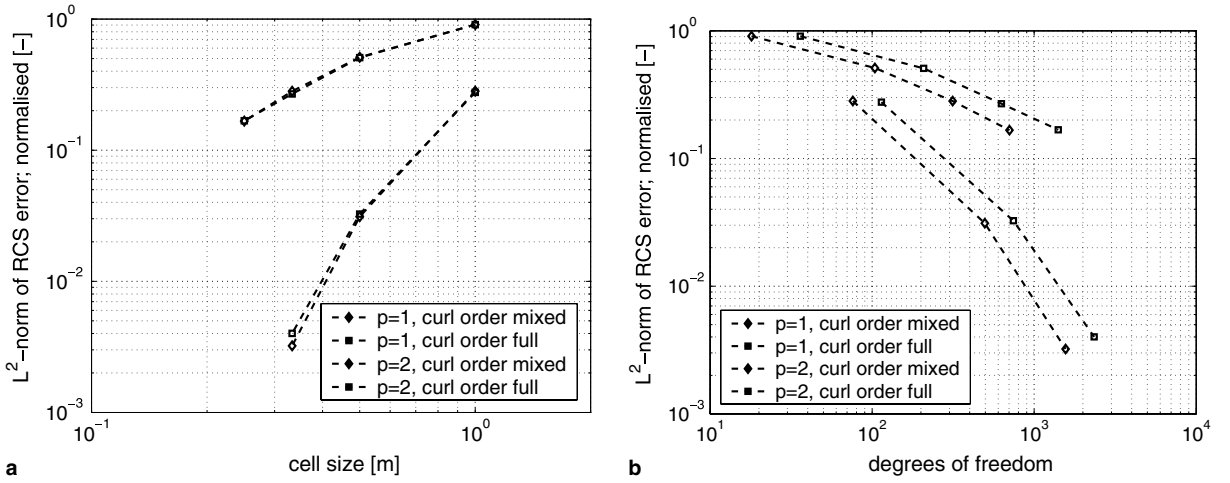

Fig. 3. RCS error convergence for formulation (21), using standard curl-conforming basis functions: (a) RCS error vs. cell size; (b) RCS error vs. degrees of freedom.

(divergence-conforming, solenoidal) modeling will not be considered when discretizing $V_{\mathrm{div},0} \times V_{\mathrm{curl}}$ and $V_{\mathrm{curl}} \times V_{\mathrm{div},0}$, since such low-order modeling does not have a counterpart in the case of the curl-conforming space.

Here, the test problem is a homogeneous unit sphere ($r_0 = 1$ m) with material parameters $\epsilon_r = 2$ and $\mu_r = 3$. The structure is exited with a plane wave at $\lambda_0 = 10$ m.

Consider formulation (24) first. Fig. 4 shows the results. It can be observed that the formulation converges as the cell size is refined. These results are very similar to those shown in Fig. 1, which can be attributed to the fact that formulation (24) is a straight-forward combination of formulations (20) and (22).

Formulation (25) is evaluated in a similar manner, and the results are shown in Fig. 5. Note again, as in the case of the dielectric results, that superior accuracy vs. degrees of freedom can be achieved with the formulation modeling curl-conforming variables (25), as compared to the one modeling divergence-conforming variables (24).

Formulations (26) and (28) are now evaluated. Since these are duals, only (26) is considered. Fig. 6 shows the results. These results are also asymptotically convergent. It is interesting to see that full-order p curl-conforming modeling performs better than does mixed-order p. This is not very surprising if one considers the following: In the formulation, the generally non-conforming representation of $\mathbf{D}/(\epsilon_r\epsilon_0)$ is projected

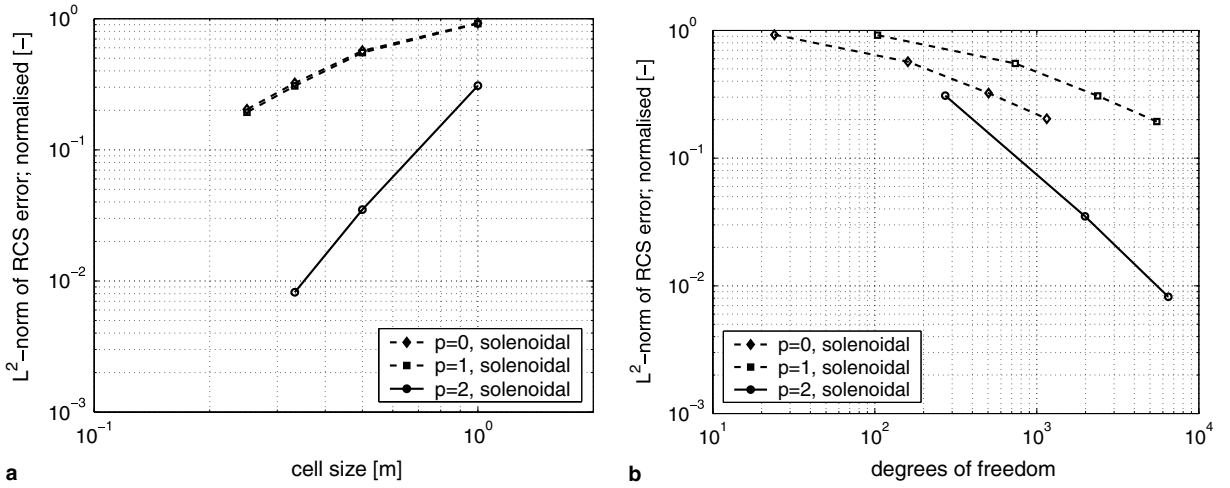

Fig. 4. RCS error convergence for formulation (24), using solenoidal divergence-conforming basis functions: (a) RCS error vs. cell size; (b) RCS error vs. degrees of freedom.

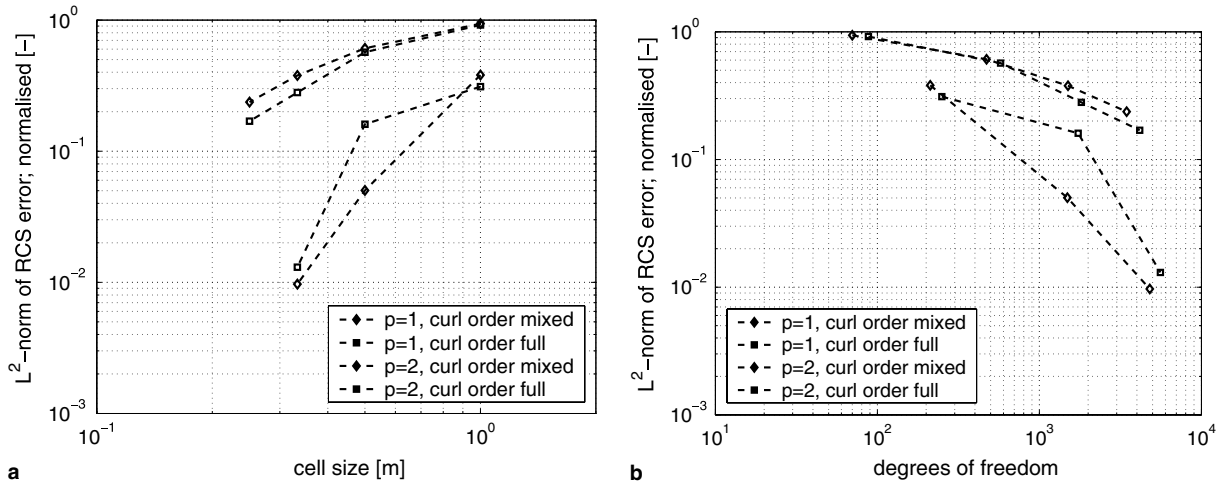

Fig. 5. RCS error convergence for formulation (25), using standard curl-conforming basis functions: (a) RCS error vs. cell size; (b) RCS error vs. degrees of freedom.

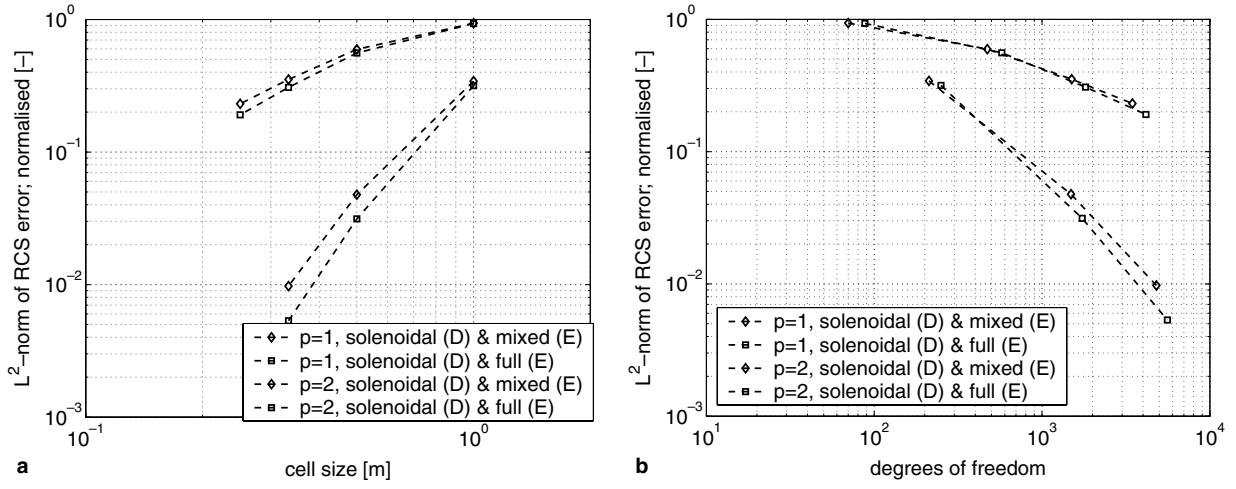

Fig. 6. RCS error convergence for formulation (26), using solenoidal divergence-conforming basis functions for **D** and curl-conforming basis functions for **E**: (a) RCS error vs. cell size; (b) RCS error vs. degrees of freedom.

onto a curl-conforming representation of **E**. On any given element K, the approximation to $\mathbf{D}/(\epsilon_r\epsilon_0)$ is solenoidal and of polynomial order p, belonging to function space $D_p^{\mathrm{sol}}(K)$; similarly, the approximation to **E** is curl-conforming to either mixed- or full polynomial order p, belonging to function spaces $C_p^{\mathrm{mixed}}(K)$ or $C_p^{\mathrm{full}}(K)$, respectively. Now, from the definitions of these spaces [18,27] it follows that $D_p^{\mathrm{sol}}(K) \not\subset C_p^{\mathrm{mixed}}(K)$, but that $D_p^{\mathrm{sol}}(K) \subset C_p^{\mathrm{full}}(K)$. Therefore, full-order modeling of **E** implies that at least on the scale of a single element, the projection can be exact, while mixed-order modeling does not.

Finally, evaluate formulations (27) and (29). Again, since these are duals, only (27) is considered. Fig. 7 shows the results. In this case, there is not a correlation between accuracy and the use of mixed- or full-oder curl-conforming modeling, as was the case in Fig. 6. The reason being that the projection is now onto the solenoidal space, which is independent of the choice of curl-conforming representation.

4.2. Scattering by a general object

Now consider scattering by the general, circularly cylindrical, inhomogeneous object shown in Fig. 8. In all cases, bistatic RCS will be shown, evaluated in the xz-plane, with incident plane wave excitation from $(\theta, \phi) =$

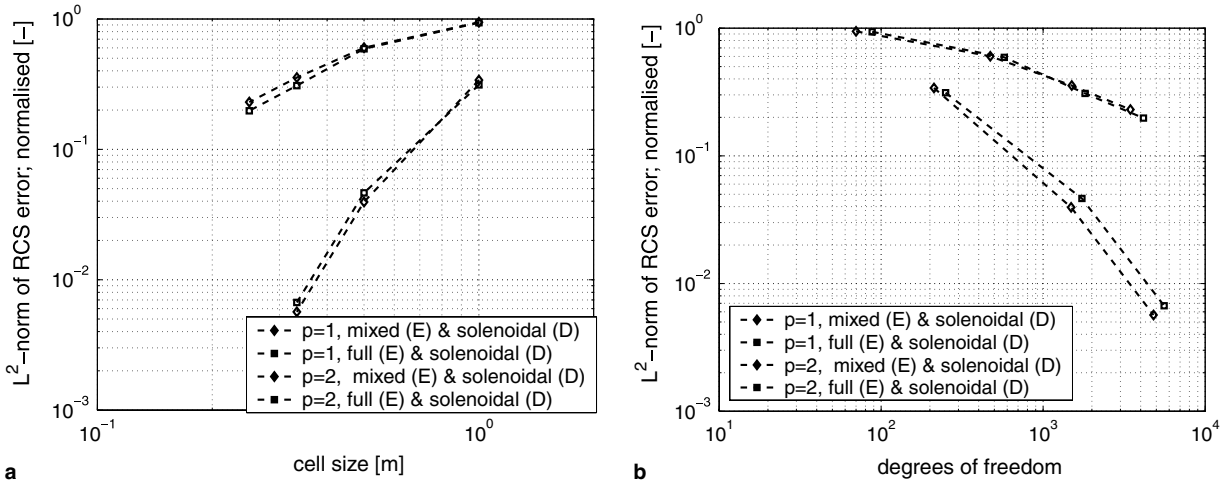

Fig. 7. RCS error convergence for formulation (27), using curl-conforming basis functions for **E** and solenoidal divergence-conforming basis functions for **D**: (a) RCS error vs. cell size; (b) RCS error vs. degrees of freedom.

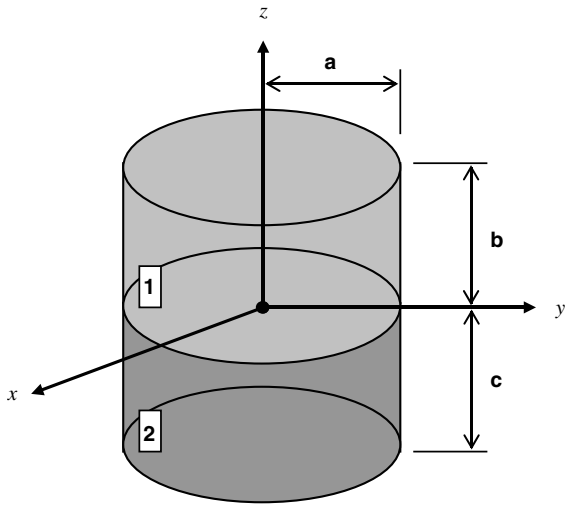

Fig. 8. Circularly cylindrical, inhomogeneous scatterer, with material parameters $\epsilon_r^{(1)}$, $\mu_r^{(1)}$, $\epsilon_r^{(2)}$ and $\mu_r^{(2)}$. Dimensions: $a = 0.1$ m, $b = 0.25$ m and $c = 0.25$ m.

(90°, 0°), with $\lambda_0 = 1$ m and $\hat{z}$-polarization of $\mathbf{E}_{\text{inc}}$. All calculations are performed on a mesh with nominal element size 0.1 m. As a reference, results are compared with a solution from a stationary, hybrid finite element-boundary integral (FE-BI) formulation [33], on a mesh which is finer by a factor of 2, employing second-order basis functions (the specific formulation used is denoted by FE-BI(S-VT) [**E**, **J**]).

Fig. 9 shows results for the dielectric case, with $\epsilon_r^{(1)} = 2 - \text{j}0.5$, $\epsilon_r^{(2)} = 3 - \text{j}1$, and $\mu_r^{(1)} = \mu_r^{(2)} = 1$. Fig. 10 shows results for the general case, with the same permittivities, but with $\mu_r^{(1)} = 4$ and $\mu_r^{(2)} = 1.5$. In all cases, solenoidal basis functions are used for $V_{\text{div},0}$, and mixed-order ones for V_{curl}, with the exception of full-order modeling of **E** in (26), for reasons noted before.

Good agreement with the reference results can be observed for all formulations, and the improvements afforded by the use of higher order basis functions are clear. All formulations yield results of similar accuracy.

4.3. Discussion

It has been shown that all formulations yield results of more or less the same accuracy, and moreover, are convergent. The question of choosing an appropriate formulation now naturally arises. The pre-existing

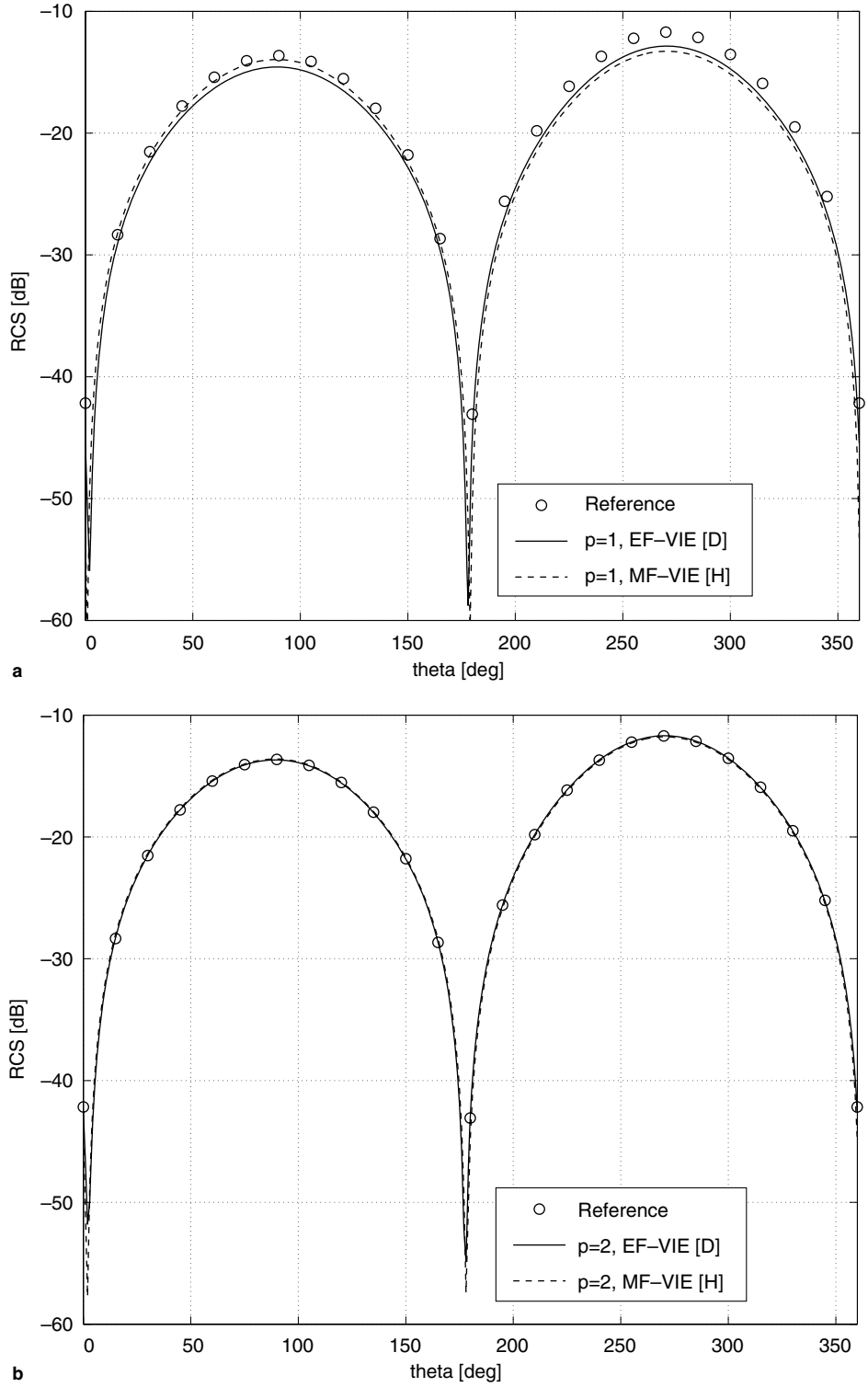

Fig. 9. Bistatic RCS of the circularly cylindrical, inhomogeneous scatterer shown in Fig. 8. Comparison between dielectric formulations: (a) first-order modeling; (b) second-order modeling.

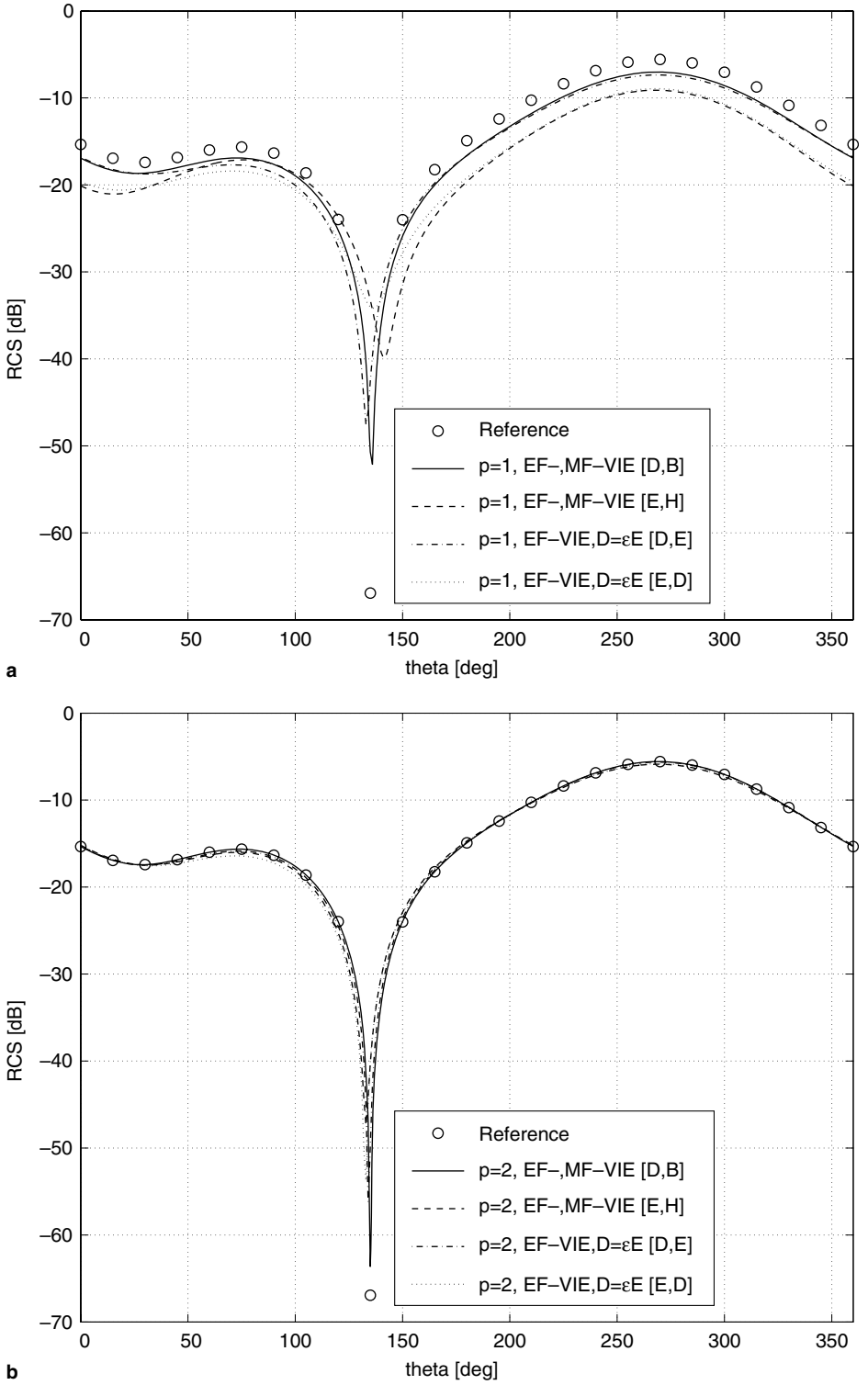

Fig. 10. Bistatic RCS of the circularly cylindrical, inhomogeneous scatterer shown in Fig. 8. Comparison between general formulations: (a) first-order modeling; (b) second-order modeling.

formulations (20), (22) and (24) are certainly viable options, but the new formulations have some distinct advantages.

In the case of dielectric or magnetic scatterers, it has already been noted that less degrees of freedom are required by the new, $\mathscr{M}(\cdot,\cdot)$ operator-based formulations (21) and (23). Also, having both EF- and MF-VIE-based formulations at hand, allows one the freedom to solve the dielectric/magnetic scatterer-problem in terms of either an electric- or magnetic field related quantity.

In the case of general scatterers, some of the new formulations have an additional advantage, apart from reducing the degrees of freedom. Consider the following matrix partitioning for the conventional formulation (24):

$$\text{Formulation G.1 (24):}\quad A = \begin{bmatrix} A_{\mathbf{D},\mathbf{D}} & A_{\mathbf{D},\mathbf{B}} \\ A_{\mathbf{B},\mathbf{D}} & A_{\mathbf{B},\mathbf{B}} \end{bmatrix}. \tag{36}$$

Each sub-matrix relates to an integral operator and is fully populated. Now consider

$$\text{Formulation G.3 (26):}\quad A = \begin{bmatrix} A_{\mathbf{D},\mathbf{D}} & A_{\mathbf{D},\mathbf{E}} \\ A_{\mathbf{E},\mathbf{D}} & A_{\mathbf{E},\mathbf{E}} \end{bmatrix}. \tag{37}$$

Here sub-matrices $A_{\mathbf{E},\mathbf{D}}$ and $A_{\mathbf{E},\mathbf{E}}$ are both highly sparse, together constituting approximately half of the system matrix. Similarly, half of the system matrices resulting from the new formulations (27)–(29) are also sparse. This property has significant implications for fast solvers, which are based on the iterative solution of the system matrix equation. With such solvers, the matrix is stored in a factored format, which requires less computer memory, and less operations for a matrix–vector product than the standard form of the matrix. With a fast solver, every sub-matrix resulting from an integral operator is usually treated separately. Thus, the use of these new formulations in conjunction with a fast solver implies a reduction in computational costs by a factor of approximately 2. Examples of fast solvers applied to the standard VIE matrix equations, and which are also applicable to the new formulations, are numerous, e.g.: the fast multipole method and its multi-level extension [34,35]; the adaptive integral method [36]; the QR-factorization method [37]; and FFT-based methods [38,39].

5. Conclusion

A comprehensive set of Galerkin projection formulations for the numerical solution of the electromagnetic VIE's was presented. This set includes pre-existing formulations, as well as a number of new ones. Results demonstrated that all formulations converge with similar accuracy in the case of a sphere-scattering test problem. It was further shown that solenoidal function spaces should be used to model electromagnetic flux densities as solution variables, in order to obtain good convergence behaviour, instead of the standard divergence-conforming spaces, which are never-the-less widely used today. To the author's knowledge, higher-order results with solenoidal discretizations were presented for the first time.

The newly proposed formulations all entail solving for some curl-conforming field(s). Such fields can be discretized with fewer degrees of freedom than the divergence-conforming solution fields used in existing approaches, implying lower computational costs for the new formulations. Moreover, some of the new formulations for generally inhomogeneous scatterers yield system matrices which are approximately half-way sparse. This means that computational costs will be down by a factor of 2 when iterative solvers are employed, which is the case for the widely-used fast methods.

Various extensions to this work are possible. To reduce implementation complexity, one could consider replacing Galerkin projection with the Nyström method described in [31]. Either way, it is very important to optimize the implementations of the volume integrals for evaluating matrix entries. Here, Gaussian quadrature in combination with Duffy's method [40] was used. Further work is needed on this subject, especially for the case of curvilinear elements. Finally, combining the efficient, new formulations with fast solvers for improved performance, has already been suggested. This applies especially to the MF-VIE based dielectric formulation (21) and EF-VIE based magnetic formulation (23), because these employ less degrees of freedom; it also applies to the half-sparse formulations for general scatterers, in which case formulations (27) and (29) are the most efficient, since both cost-reduction mechanisms feature to maximum

benefit. Note that when combined with a fast solver, the VIE-based formulations compare quite favorably with FE- and FE-BI formulations in terms of computational cost scaling, especially when taking into account that the FE-based formulations suffer from dispersion errors, while the VIE-based formulations do not.

Acknowledgment

The author would like to acknowledge useful discussions with David B. Davidson (University of Stellenbosch, South Africa).

References

[1] D.H. Schaubert, D.R. Wilton, A.W. Glisson, A tetrahedral modeling method for electromagnetic scattering by arbitrary shaped inhomogeneous dielectric bodies, IEEE Trans. Antennas Propagat. 32 (1) (1984) 77–85.
[2] J.J.H. Wang, Generalized Moment Methods in Electromagnetics, John Wiley, New York, 1991.
[3] E.K. Miller, L. Medgyesi-Mitschang, E.H. Newman (Eds.), Computational Electromagnetics: Frequency Domain Method of Moments, IEEE Press, New York, 1992.
[4] K. Lumme, J. Rahola, Comparison of light scattering by stochastically rough spheres, best-fit spheroids and spheres, J. Quant. Spectrosc. Radiat. Transfer 60 (3) (1998) 439–450.
[5] L. Tsang, K.H. Ding, S.E. Shih, J.A. Kong, Scattering of electromagnetic waves from dense distributions of spheroidal particles based on Monte Carlo simulations, J. Opt. Soc. Am. A 15 (10) (1998) 2660–2669.
[6] K. Tanaka, M. Tanaka, Optimized computer-aided design of I-shaped subwavelength aperture for high intensity and small spot size, Opt. Commun. 233 (2004) 231–244.
[7] K. Tanaka, M. Tanaka, Analysis and numerical computation of diffraction of an optical field by a subwavelength-size aperture in a thick metallic screen by use of a volume integral equation, Appl. Opt. 43 (8) (2004) 1734–1746.
[8] J. Avelin, R. Sharma, I. Hänninen, A.H. Sihvola, Polarizability analysis of cubical and square-shaped dielectric scatterers, IEEE Trans. Antennas Propagat. 49 (3) (2001) 451–457.
[9] C.C. Lu, Indoor radio-wave propagation modeling by multilevel fast multipole algorithm, Microwave Opt. Technol. Lett. 29 (3) (2001) 168–175.
[10] W.C. Chew, J.-M. Jin, E. Michielssen, J. Song (Eds.), Fast and Efficient Algorithms in Computational Electromagnetics, Artech House, Boston, 2001.
[11] C.C. Lu, W.C. Chew, A coupled surface-volume integral equation approach for the calculation of electromagnetic scattering from composite metallic and material targets, IEEE Trans. Antennas Propagat. 48 (12) (2000) 1866–1868.
[12] L.S. Mendes, S.A. Carvalho, Scattering of EM waves by homogeneous dielectrics with the use of the method of moments and 3D solenoidal basis functions, Microwave Opt. Technol. Lett. 12 (6) (1996) 327–331.
[13] S. Kulkarni, R. Lemdiasov, R. Ludwig, S. Makarov, Comparison of two sets of low-order basis functions for tetrahedral VIE modeling, IEEE Trans. Antennas Propagat. 52 (10) (2004) 2789–2794.
[14] I.-T. Chiang, W.-C. Chew, New formulation and iterative solution for low-frequency volume integral equation, J. Electromagn. Waves Appl. 19 (3) (2005) 289–306.
[15] A.F. Peterson, A magnetic field integral equation formulation for electromagnetic scattering from inhomogeneous 3D dielectric bodies, in: Proceedings of the 5th Annual Review of Progress in Applied Computational Electromagnetics, Monterey, CA, 1989, pp. 387–403.
[16] J.L. Volakis, Alternative field representations and integral equations for modeling inhomogeneous dielectrics, IEEE Trans. Microwave Theory Technol. 40 (3) (1992) 604–608.
[17] J.M. Hyman, M. Shashkov, Mimetic discretizations for Maxwell's equations, J. Comput. Phys. 151 (1999) 881–909.
[18] M.M. Botha, Fully hierarchical divergence-conforming basis functions on tetrahedral cells with some applications, submitted for publication.
[19] J.P. Webb, Hierarchal vector basis functions of arbitrary order for triangular and tetrahedral finite elements, IEEE Trans. Antennas Propagat. 47 (8) (1999) 1244–1253.
[20] C.A. Balanis, Advanced Engineering Electromagnetics, John Wiley, New York, 1989.
[21] J. Van Bladel, Singular Electromagnetic Fields and Sources, Oxford University Press, Oxford, 1991.
[22] K.E. Atkinson, The Numerical Solution of Integral Equations of the Second Kind, Cambridge University Press, Cambridge, UK, 1997.
[23] A. Ishimaru, Electromagnetic Wave Propagation, Radiation, and Scattering, Prentice-Hall, Englewood Cliffs, NJ, 1991.
[24] J.P. Kottman, O.J.F. Martin, Accurate solution of the volume integral equation for high-permittivity scatterers, IEEE Trans. Antennas Propagat. 48 (11) (2000) 1719–1726.
[25] R. Scheichl, Decoupling three-dimensional mixed problems using divergence-free finite elements, SIAM J. Sci. Comput. 23 (5) (2002) 1752–1776.
[26] W.G. Strang, G.J. Fix, An Analysis of the Finite Element Method, Wellesley Cambridge, Cambridge, UK, 1973.
[27] J.C. Nédélec, A new family of mixed finite elements in $\Re^3$, Numer. Math. 50 (1986) 57–81.

[28] R. Hiptmair, Canonical construction of finite elements, Math. Comput. 68 (228) (1999) 1325–1346.
[29] J. Rahola, On the eigenvalues of the volume integral operator of electromagnetic scattering, SIAM J. Sci. Comput. 21 (5) (2000) 1740–1754.
[30] R. Kress, Linear Integral Equations, second ed., Applied Mathematical Sciences, 82, Springer-Verlag, New York, 1999.
[31] L.F. Canino, J.J. Ottusch, M.A. Stalzer, J.L. Visher, S.M. Wandzura, Numerical solution of the Helmholtz equation in 2D and 3D using a high-order Nyström discretization, J. Comput. Phys. 146 (1998) 627–663.
[32] D.B. Davidson, An evaluation of mixed-order versus full-order vector finite elements, IEEE Trans. Antennas Propagat. 51 (9) (2003) 2430–2441.
[33] M.M. Botha, J.-M. Jin, On the variational formulation of hybrid finite element-boundary integral techniques for electromagnetic analysis, IEEE Trans. Antennas Propagat. 52 (11) (2004) 3037–3047.
[34] C.-C. Lu, A fast algorithm based on volume integral equation for analysis of arbitrarily shaped dielectric radomes, IEEE Trans. Antennas Propagat. 51 (3) (2003) 606–612.
[35] K. Sertel, J.L. Volakis, Multilevel fast multipole method solution of volume integral equations using parametric geometry modeling, IEEE Trans. Antennas Propagat. 52 (7) (2004) 1686–1692.
[36] W.-B. Ewe, L.-W. Li, M.-S. Leong, Fast solution of mixed dielectric/conducting scattering problem using volume-surface adaptive integral method, IEEE Trans. Antennas Propagat. 52 (11) (2004) 3071–3077.
[37] N.A. Ozdemir, J.-F. Lee, A low-rank IE-QR algorithm for matrix compression in volume integral equations, IEEE Trans. Magn. 40 (2) (2004) 1017–1020.
[38] P. Zwamborn, P.M. Van den Berg, The three-dimensional weak form of the conjugate gradient FFT method for solving scattering problems, IEEE Trans. Microwave Theory Technol. 40 (9) (1992) 1757–1766.
[39] Z.Q. Zhang, Q.H. Liu, Three dimensional weak-form conjugate- and biconjugate-gradient FFT methods for volume integral equations, Microwave Opt. Technol. Lett. 29 (5) (2001) 350–356.
[40] M.G. Duffy, Quadrature over a pyramid or cube of integrands with a singularity at a vertex, SIAM J. Numer. Anal. 19 (6) (1982) 1260–1262.